


## Article

# Experimental Study on the Mechanical Properties of Recycled Spiral Steel Fiber-Reinforced Rubber Concrete

Jinqiu Yan <sup>1</sup>, Yongtao Gao <sup>2,\*</sup>, Minggao Tang <sup>2</sup>, Nansheng Ding <sup>2</sup>, Qiang Xu <sup>2</sup>, Man Peng <sup>2</sup> and Hua Zhao <sup>2</sup> 

<sup>1</sup> School of Architecture and Civil Engineering, Xihua University, Jinzhou Road 999#, Chengdu 610039, China; shang1597533@163.com

<sup>2</sup> State Key Laboratory of Geohazard Prevention and Geoenvironment Protection, No. 1, East Third Road, Erxianqiao, Chengdu 610059, China; tomyr2008@163.com (M.T.); dingnansheng@cdut.edu.cn (N.D.); xuqiang\_68@126.com (Q.X.)

\* Correspondence: gaoyongtao06@cdut.edu.cn

**Abstract:** Recycled rubber (RR) and recycled spiral steel fiber (RSSF) were added to plain concrete (PC) to prepare recycled spiral steel fiber rubber concrete (SSFRC) with matrix strengths of C30, C40, and C50. Strength tests on the PC, rubber concrete (RC), and SSFRC were carried out, including the cube compressive strength, splitting tensile strength, and flexural strength. The effects of RSSF and RR on the mechanical properties of concrete were analyzed. Simultaneously, the stress–strain curve of the SSFRC was obtained through axial compressive testing, and the toughness of SSFRC was evaluated by three indexes: the tensile compression ratio, bending compression ratio, and toughness index. The results show that adding RR to PC results in a decrease in the mechanical properties of concrete with different matrix strengths, and the addition of RSSF can make up for the strength loss of the rubber. The mechanical strength of SSFRC with different matrix strengths increased first and then decreased with the increase in RSSF content. The cubic compressive strength reached its peak value when the content of RSSF was 1%, and the splitting tensile strength and flexural strength reach their peak values when the content of RSSF was 1.5%. RSSF works best with rubber particles at the right dosage to further increase the toughness of the concrete. When the rubber content is 10%, and the RSSF content is 1.5%, the mechanical strength enhancement effect of SSFRC is at its best, and the toughness is also at its best.

**Keywords:** recycled spiral steel fiber rubber concrete; strength test; reinforcement; toughness



**Citation:** Yan, J.; Gao, Y.; Tang, M.; Ding, N.; Xu, Q.; Peng, M.; Zhao, H.

Experimental Study on the Mechanical Properties of Recycled Spiral Steel Fiber-Reinforced Rubber Concrete. *Buildings* **2024**, *14*, 897.

<https://doi.org/10.3390/buildings14040897>

Academic Editors: Dan Bompa and Cedric Payan

Received: 3 January 2024

Revised: 2 March 2024

Accepted: 22 March 2024

Published: 26 March 2024



**Copyright:** © 2024 by the authors. Licensee MDPI, Basel, Switzerland. This article is an open access article distributed under the terms and conditions of the Creative Commons Attribution (CC BY) license (<https://creativecommons.org/licenses/by/4.0/>).

## 1. Introduction

With the rapid development of the global transportation industry, hundreds of millions of discarded tires are produced by the elimination of vehicles every year [1,2]. According to statistics, about 50 million tires are directly discarded every year, with only a small portion able to be recycled, and 500 million tires will be discarded by 2030 [3,4]. A landfill of waste tires can cause serious fire hazards and environmental pollution, and the accumulated tires can also harbor bacteria that can cause diseases in humans [5–7]. The existing pyrolysis treatment measures for waste tires not only have a long investment return cycle but also produce a large amount of carbon dioxide, which promotes the greenhouse effect of the atmosphere to a certain extent [8]. In order to maximize the recycling of waste tires and reduce their harm to the environment and society, waste tires can be made into rubber particles instead of natural sand so as to partially replace the fine aggregate in concrete and achieve the purpose of saving resources [9].

B.S. Thomas et al. [10] added waste tire rubber particles to concrete and studied the fatigue performance of rubber concrete under constant amplitude cyclic loading, finding that the fatigue performance of rubber concrete is better than that of ordinary concrete. Han Q. et al. [11] found that when the rubber particle size and content reached the optimum, the performance of concrete under cyclic load could be effectively improved, making it

suitable for the construction of rigid pavement. P.N. Pham et al. [12] added waste rubber particles to high-strength concrete, and the results showed that the impact resistance of concrete increased by 83%. Hassanli R. et al. [13] added modified waste rubber particles to recycled aggregate concrete, and its impact resistance increased significantly compared with recycled aggregate concrete. O. Youssf et al. [14] found that rubber particles at a specific particle size and dosage could enhance the freeze-thaw resistance of concrete. T.M. Pham et al. [15] found that modified recycled rubber particles can improve the vibration reduction and sound insulation ability of light aggregate concrete.

Due to its low strength and low elastic modulus, rubber will reduce the mechanical properties of concrete [16–18]. In order to improve this strength loss, the current main methods are to modify the rubber surface, add other fiber materials, etc. [19]. G.A. Issa et al. [20] optimized the mix ratio of rubber concrete, and the loss of its force-flow and mechanical properties was limited. K. Shahzad et al. [21] et al. studied the surface changes of NaOH- and urea-modified rubber. Both materials reduced the hydrophobicity of the rubber surface to varying degrees. NaOH treatment can remove part of the hydrophobic substances on the surface of rubber particles, increase the surface roughness and surface area of rubber particles, and slightly reduce the water contact angle of rubber, where the reduced rubber water contact angle is  $36.9^\circ$ . The treatment method is simple to operate and low in cost. Z. Keshavarz et al. [22] treated rubber particles with NaOH, silane coupling agent (SCA), and a sulfuric acid solution, and the mechanical properties of the rubber concrete were significantly enhanced. In addition to fiber materials, at present, the best effect is mainly from adding steel fiber to rubber concrete. M.K. Ismail et al. [23] added steel fiber to waste rubber concrete and found that the synergistic effect of the steel fiber and rubber could improve the compressive strength of the concrete. I. Guerra et al. [24] found that steel fiber could significantly enhance the dynamic and static tensile strength of concrete, and its ductility was also significantly improved. H. Gharibi, D.G. Aggelis, and J. Xu et al. [25–27] showed that the combination of steel fiber and rubber particles yielded a significant improvement in the tensile properties. The addition of steel fiber can also reduce the loss of flexural strength, and the crack width of steel fiber rubber concrete is much smaller than that of steel fiber concrete. Q. Han and J. Xu et al. [28–30] found that the combination of waste rubber and steel fiber can further improve the toughness of concrete, and the synergistic effect of the two can greatly increase the fracture mode of concrete. A.A. Abouhussien et al. [31] believed that steel fiber orientation could improve the flexural strength and crack resistance of concrete. Z. Keshavarz, D. and M.S.S. Ahamad et al. [32,33] added steel fiber to rubber concrete, and the peak deflection, toughness, and ductility of the rubber concrete under bending and shearing all increased with the increase in steel fiber content. J. Xu and L.A. Jimoda et al. [34,35] found that the bending strength and tensile strength were related to the steel fiber content, and the strain, hardening, and softening behaviors of steel fiber rubber concrete were mainly affected by the steel fiber content.

In current research methods, primary steel fibers or steel fibers extracted from waste tires are mainly used to reinforce rubber concrete, but these steel fibers have a planar shape. Spiral-shaped recycled steel fibers have a three-dimensional spatial shape, which can form a three-dimensional bonding structure with rubber and concrete and have obvious spatial mechanical characteristics. They can form bonds with concrete in multiple dimensions, thereby preventing concrete from bonding in multiple directions. In order to explore the influence of spiral recycled steel fiber on rubber concrete, this experiment adopts the basic mechanical properties of recycled spiral steel fiber-reinforced rubber concrete with different volume contents. We study the cube compressive strength, splitting tensile strength, flexural strength, and prismatic axial compressive strength of various SSFRCs at 28 d. At the same time, the tensile compression ratio, folding compression ratio, and toughness index were used to evaluate the toughness of RSSFRC, and the measured values of the axial compressive strength and cubic compressive strength of SSFRC were fitted, while a more suitable formula for calculating the axial compressive strength of RSSFRC was established. Through the experimental research of RSSFRC, the three-dimensional model

mechanism of the improvement of the mechanical properties of rubber concrete by recycled spiral steel fibers was revealed, and the ductility working mechanism of recycled spiral steel fiber rubber concrete was explored. This provides a new approach for the utilization of renewable resources and the green application of civil engineering materials.

## 2. Materials and Test Methods

### 2.1. Materials

Common Portland cement P.O 42.5 was used as the test cement. The packing density was  $3.05 \times 10^3 \text{ kg/m}^3$ , and its related performance indexes are shown in Table 1. The coarse aggregate was gravel with a particle size  $d < 40 \text{ mm}$ , and the packing density was  $2.5 \times 10^3 \text{ kg/m}^3$ . The fine aggregate was medium coarse sand with an apparent density of  $2.65 \text{ kg/cm}^3$ , and ordinary tap water was used for mixing, with the particle size range of the sand being between 0.5 and 2.0 mm. The RSSF came from the residual material of machining, and its density was  $7.8 \times 10^3 \text{ kg/m}^3$ . It had a three-dimensional helical structure with an average length of 20~40 mm, a width from 2 to 4 mm, a thickness of less than 0.5 mm, an average tensile strength of no less than 350 MPa, and an elastic modulus of  $2.1 \times 10^5 \text{ N/mm}^2$ . The rubber came from the broken particles of waste tires, where the packing density was  $0.9 \times 10^3 \text{ kg/m}^3$ , the particle size was from 1 to 3 mm, and it was washed with 5% NaOH solution to  $\text{pH} = 7$ . The raw materials are shown in Figure 1.

**Table 1.** Cement performance index.

Standard Consistency (%)	Setting Time (min)		Compressive Strength of Cube (MPa)		Flexural Strength (MPa)	
	Initial condensation	Termination condensation	3 d	28 d	3 d	28 d
24.2	180	260	25.5	52.5	5.2	8.8

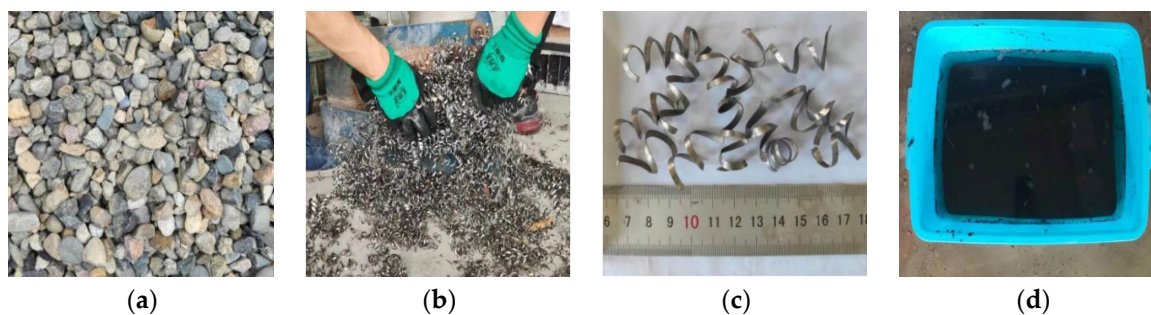


**Figure 1.** Raw materials for testing: (a) coarse aggregate; (b) RSSF inspection; (c) treated RSSF; and (d) alkali washed rubber.

### 2.2. Specimen Making and Maintenance

According to the existing research results and the actual situation of this test, the rubber content was determined to be 10%, replacing fine aggregate sand with rubber at a volume content of 10% sand. The volume content of the RSSF was 0%, 0.5%, 1.0%, 1.5%, and 2%. The matrix strength of the SSFRC specimens was C30, C40, and C50. The concrete mix ratios of the specimens with different strength grades are shown in Table 2. Since the design strength of all concrete specimens was between C30 and C60, non-standard specimen sizes were used in all kinds of tests. For details on the size of the test blocks, see Table 3.

Table 2. Mix ratio of each specimen.

Strength Grade of Concrete Matrix	RSSF Volume Content (%)	Amount of Each Material per Unit Volume (kg/m <sup>3</sup> )					
		Cement	Gravel	Sand	Water	Rubber	RSSF
C30	0	380	1251	644	180	0	0
	0	380	1251	580	180	32	0
	0.5	380	1251	580	180	32	39
	1	380	1251	580	180	32	79
	1.5	380	1251	580	180	32	118
	2	380	1251	580	180	32	157
C40	0	420	1241	577	180	0	0
	0	420	1241	519	180	28	0
	0.5	420	1241	519	180	28	39
	1	420	1241	519	180	28	79
	1.5	420	1241	519	180	28	118
	2	420	1241	519	180	28	157
C50	0	470	1200	617	165	0	0
	0	470	1200	555	165	30	0
	0.5	470	1200	555	165	30	39
	1	470	1200	555	165	30	79
	1.5	470	1200	555	165	30	118
	2	470	1200	555	165	30	157

Table 3. Test specimen.

Intensity Type	Specimen Size (mm)	Number of Specimens	Number per Group	Total	Total
Compressive strength of cube	100 × 100 × 100	18	3	54	
Splitting tensile strength	100 × 100 × 100	18	3	54	
Flexural strength	100 × 100 × 400	18	3	54	216
Axial compressive strength	100 × 100 × 300	18	3	54	

When the specimen was made, it was carried out in strict accordance with the specification of “steel fiber reinforced concrete (JG/T472-2015)”, and the raw materials required for weighing were reserved. First, we poured the coarse aggregate gravel, fine aggregate river sand, and cement into the raw materials on an impervious steel plate that was soaked in advance and dry mixed for 2 min. After the dry mixing, we evenly sprinkled the rubber particles and continued to stir it. After fully mixing, we added water and then the RSSF. The whole process of adding RSSF had to include stirring, and the RSSF had to be input three times. When each RSSF was input, we waited for the previous batch of RSSF to be fully and evenly mixed with the mixture. With the increase in RSSF content, the input times of the RSSF could be appropriately increased, and the wet mixing time was not less than 3 min. The resulting SSFRC mixture was subjected to slump testing to evaluate its workability. Then, the SSFRC mixture was poured into a clean mold coated with waste oil, and the shaking table was used to vibrate and compact the mixture until the surface of the mix was slurry, and a small amount of waste oil was spilled. When the vibration was over, we smoothed and removed air bubbles with a scraper. The mold was removed 24 h after casting and placed in water at  $20 \pm 2$  °C for maintenance for 28 d.

### 2.3. Test Method

#### 2.3.1. Slump

The slump test could be carried out after the SSFRC mixture was evenly mixed, Relevant test operations were carried out in accordance with the “steel fiber reinforced concrete (JG/T472-2015)” of China.



### 2.3.2. Mechanical Strength

The compressive strength of the cube was tested with a WHY-1000 microcomputer controlled pressure testing machine with a maximum measuring range of 1000 kN. The splitting tensile strength was tested with a CSS-555000 microcomputer controlled electro-hydraulic servo testing machine, which was combined with a steel splitting tensile fixture. The flexural strength was measured with a YA-500 microcomputer hydraulic pressure testing machine. The axial compression strength was tested with a CSS-MAM600DL electro-hydraulic servo universal testing machine. The relevant test operation and strength calculations were carried out in accordance with the “Fiber Concrete Test Method Standard”, and the test equipment and installation are shown in Figure 2.

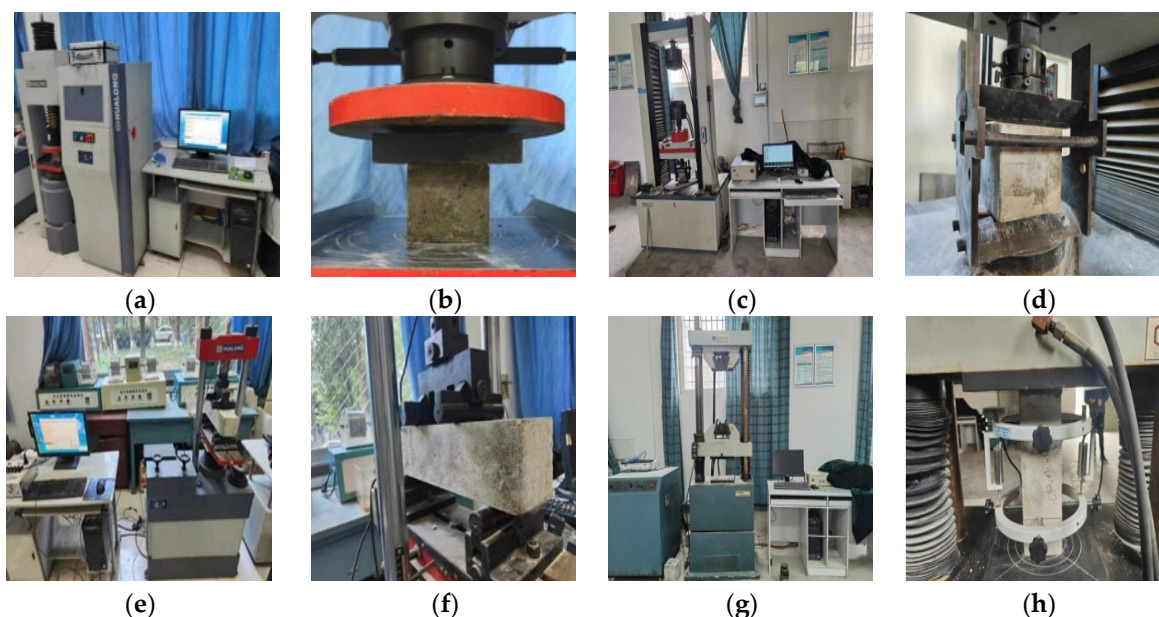


**Figure 2.** Installation diagram of test equipment and specimens: (a) WHY-1000 testing machine; (b) installation diagram of compressive strength testing machine; (c) CSS-555000 testing machine; (d) installation diagram of tensile strength testing machine; (e) YA-500 testing machine; (f) installation drawing of flexural strength testing machine; (g) CSS-MAM600DL testing machine; and (h) installation drawing of axial compression testing machine.

## 3. Test Results and Discussion

### 3.1. Slump

Figure 3 shows the variation trend of the slump values of concrete with different strengths. Table 4 shows the slump values of the PC, RC, and SSFRC mixes with different volumes. As can be seen in Figure 3, the addition of rubber particles and steel fibers reduced the slump of the concrete to a certain extent, making its working performance worse. The higher the RSSF content was, the more the slump would be reduced. The higher the strength of the concrete matrix, the lower the slump.

The reason for the above phenomenon is that the surface of the rubber particles after alkali washing was uneven, and the shape was irregular, which enhanced the water absorption capacity of the rubber surface and increased the friction force of the internal flow of the mix, thereby reducing the fluidity of the mix. The RSSF used in the test had a three-dimensional helical structure and good spatial characteristics, and the particles were connected to each other in the concrete, which enhanced the internal connection of the concrete, increased the friction force of the internal flow of the concrete mix, and restricted the movement of each. The slump of the mixture was decreased by the synergistic effect of the RSSF and rubber. This is because the addition of a large amount of RSSF makes the RSSF occasionally cross, and it cannot significantly bridge the effect, forming a network structure.

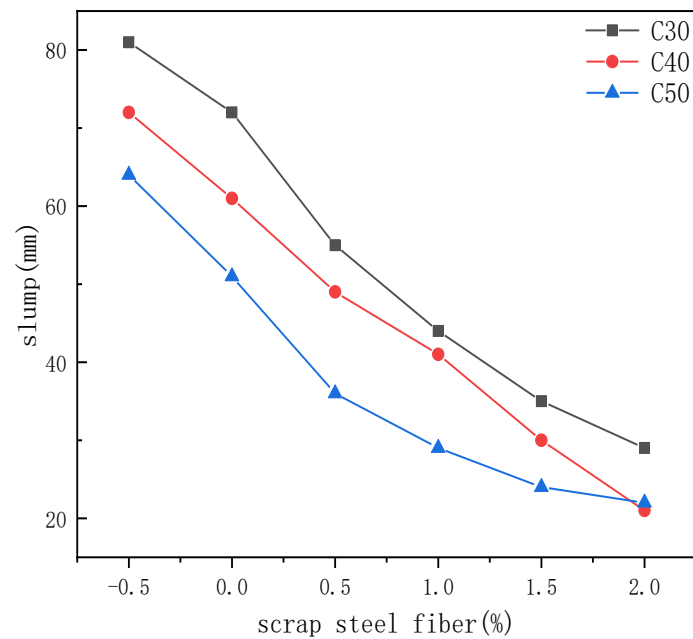


**Figure 3.** Slump test results.

**Table 4.** Slump values of concrete with different strengths.

Specimen Number	Slump (mm)
C30—PC	81
C30—RC	72
C30—SSFRC—0.5%	55
C30—SSFRC—1.0%	44
C30—SSFRC—1.5%	35
C30—SSFRC—2.0%	29
C40—PC	72
C40—RC	61
C40—SSFRC—0.5%	49
C40—SSFRC—1.0%	41
C40—SSFRC—1.5%	30
C40—SSFRC—2.0%	21
C50—PC	64
C50—RC	51
C50—SSFRC—0.5%	36
C50—SSFRC—1.0%	29
C50—SSFRC—1.5%	24
C50—SSFRC—2.0%	22

### 3.2. Mechanical Strength

Figure 4 shows the variation trend of the mechanical strength of the PC, RC, and SSFRC with different strengths at 28 d, including the cube compressive strength, splitting tensile strength, flexural strength, and axial compressive strength.

As can be seen in Figure 4, after adding 10% rubber particles to the PC, the mechanical strength of the RC decreased to varying degrees. The cubic compressive strength, splitting tensile strength, and flexural strength of the C30 concrete decreased by about 10%. Those of the C40 concrete decreased by about 14%, while those of the C50 concrete decreased by about 21%. This shows that the addition of rubber has the same influence on the mechanical strength of concrete with the same matrix strength, and the influence on the mechanical properties of high-strength concrete is greater when the matrix strength is different.

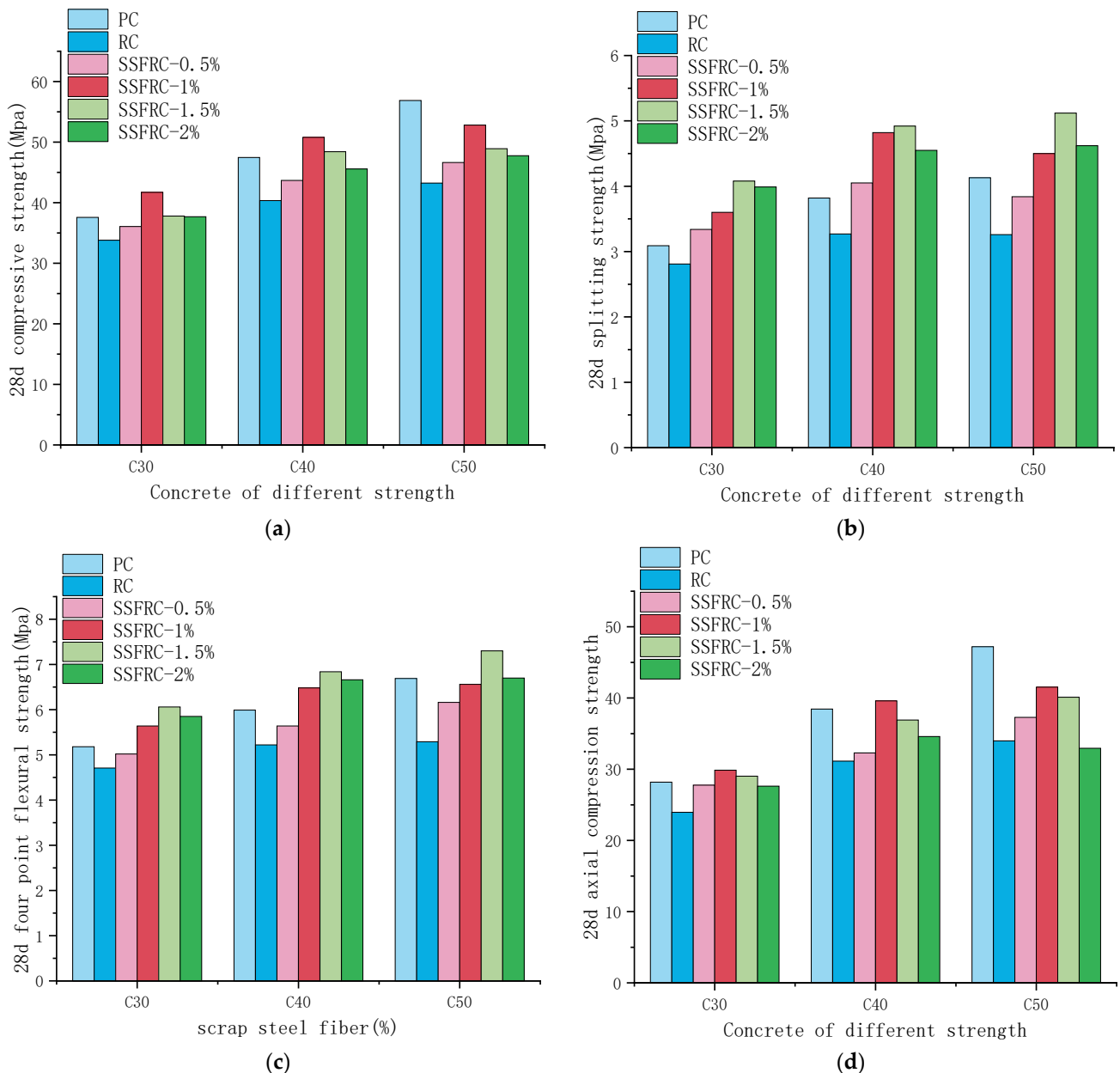


**Figure 4.** Strength variation trends of different types of concrete: (a) cube compressive strength; (b) splitting tensile strength; (c) flexural strength; and (d) axial compressive strength.

The reason for this result is that the structural weakness of the rubber itself, as well as the hydrophobicity of the rubber particles after alkali washing, made the interface transition zone between the rubber particles and the cement stone clear. Studies have shown that the strength of the interface area between rubber and mortar is only 35% of the strength of mortar [36–38], and the surface of rubber particles cannot become completely hydrophilic with this alkaline washing treatment [39,40]. The hydrophobicity of rubber particles will prevent water molecules from contacting the rubber surface, thus inhibiting the hydration of cement on the rubber surface, resulting in a reduction in calcium silicate hydrate (C-S-H) gel, the hydration product of the main strength source in RC, and a reduction in compressive strength [41–43].

It can also be seen in Figure 4 that after adding RSSF, the mechanical strength of concrete with different matrix strengths presented a trend of first increasing and then decreasing with the increase in RSSF content. The compressive strength of SSFRC with different matrix strengths reached its peak value when the content of RSSF was 1%. The

peak compressive strength of the C30 and C40 concrete increased by 23% and 26% compared with the RC, respectively, with both exceeding that of plain PC. The peak compressive strength of the C50 concrete increased by 22% compared with the RC but only reached 93% of the RC's strength. The splitting tensile strength and flexural strength both reached their peak values when the content of RSSF was 1.5%. Compared with the RC, the peak tensile strengths of the C30, C40, and C50 concrete increased by 45%, 50%, and 56%, respectively, all exceeding that of the PC. The corresponding peak bending strength increased by 28%, 31%, and 37% compared with the RC, respectively, which also exceeded that of the PC.

Figure 5 shows three mechanical strength ratios of different types of concrete, including the cube compressive strength ratio, splitting tensile strength ratio, and flexural strength ratio. Table 5 shows the 28 d mechanical strengths of the PC, RC, and SSFRC.

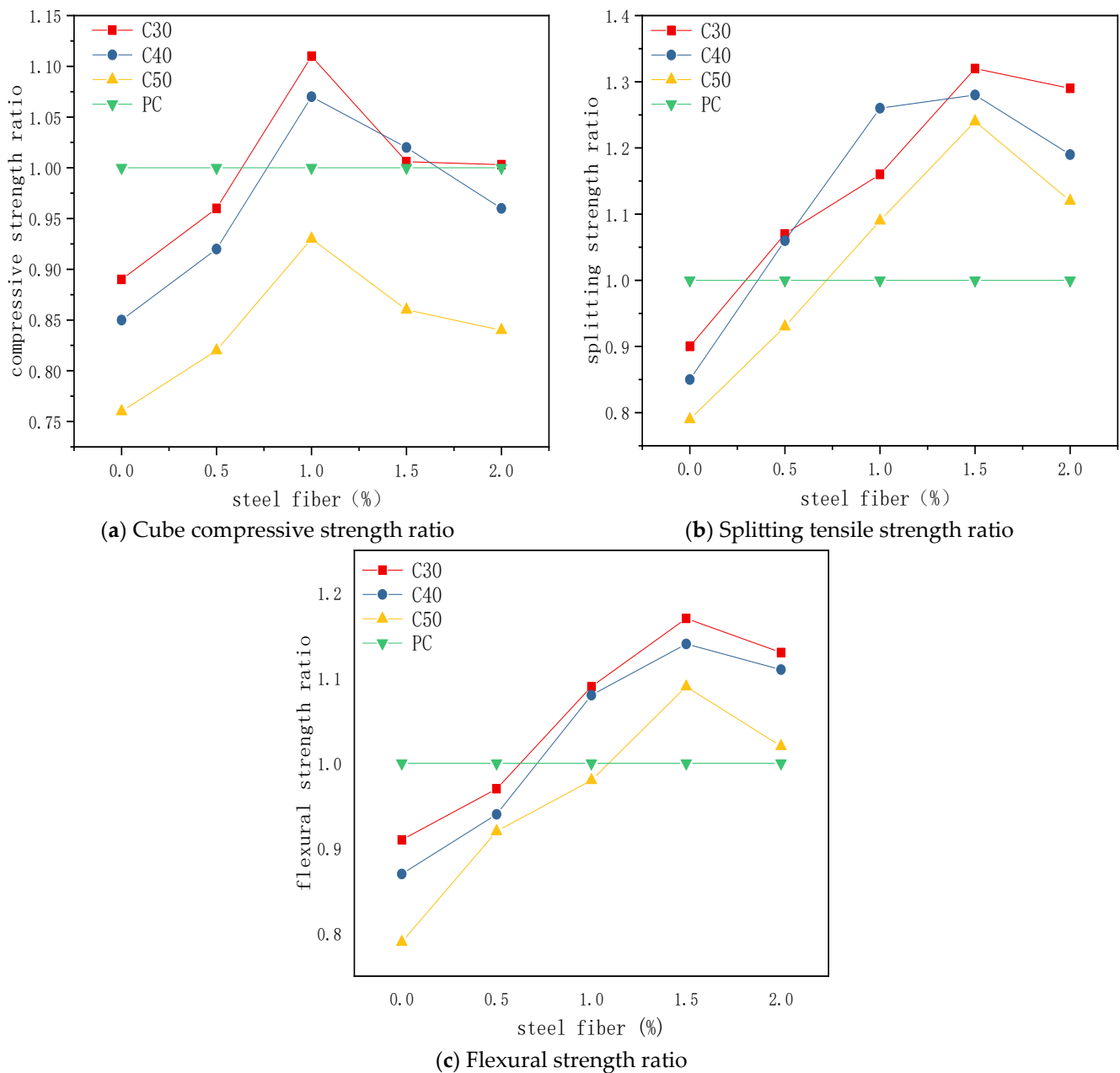


**Figure 5.** Mechanical strength ratios of different types of concrete: (a) cube compressive strength ratio; (b) splitting tensile strength ratio; and (c) flexural strength ratio.



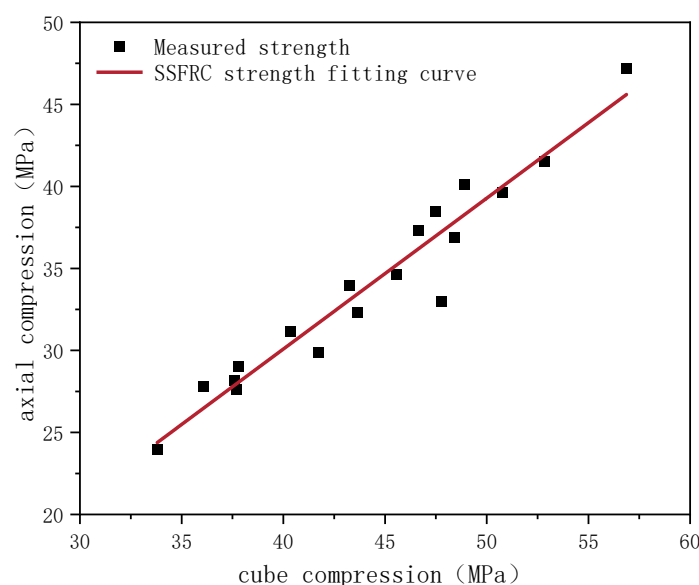
**Table 5.** Different types of concrete mechanical strength values at 28 d.

Specimen Number	Compressive Strength of Cube (MPa)	Splitting Tensile Strength (MPa)	Flexural Strength (MPa)	Axial Compressive Strength (MPa)
C30-PC	37.58	3.09	5.18	28.18
C30-RC	33.8	2.81	4.71	23.95
C30-SSFEC-0.5%	36.07	3.34	5.02	27.77
C30-SSFEC-1%	41.71	3.6	5.64	29.87
C30-SSFEC-1.5%	37.8	4.08	6.06	29.03
C30-SSFEC-2%	37.69	3.99	5.85	27.62
C40-PC	47.47	3.82	5.99	38.45
C40-RC	40.35	3.27	5.22	31.14
C40-SSFEC-0.5%	43.67	4.05	5.64	32.29
C40-SSFEC-1%	50.79	4.82	6.48	39.6
C40-SSFEC-1.5%	48.42	4.92	6.84	36.91
C40-SSFEC-2%	45.57	4.55	6.66	34.60
C50-PC	56.87	4.13	6.69	47.2
C50-RC	43.23	3.26	5.29	33.98
C50-SSFEC-0.5%	46.63	3.84	6.16	37.28
C50-SSFEC-1%	52.82	4.50	6.56	41.53
C50-SSFEC-1.5%	48.92	5.12	7.30	40.12
C50-SSFEC-2%	47.76	4.62	6.70	32.95

It can be seen in Figure 5 that the mechanical strength of the C30, C40, and C50 SSFRC increased compared with the PC. In addition to the C50 cube compressive strength being lower than that of the PC, the rest exceeded that of the PC. According to the data in Figure 5, it can be seen that the addition of RSSF could greatly improve the tensile and flexural strength of RC, but the improvement in compressive strength was not obvious. Moreover, 1% RSSF had the best effect on the cube compressive strength, and the 1.5% RSSF had the best effect on the splitting tensile strength and flexural strength.

The ratio of the axial compressive strengths and cube compressive strengths of different kinds of concrete was different, and the ratio of the two was between 0.69 and about 0.83 in this test. Based on the measured values of the axial compressive strength and cube compressive strength, a new calculation relationship suitable for SSFRC was fitted [44–46], as shown in Equation (1), and the relationship between the two is shown in Figure 6:

$$f_c = 0.92f_{cu} - 6.72 \quad (1)$$

**Figure 6.** Relationship between SSFRC cube compression and axial compression.

In Equation (1),  $f_c$  is the axial compressive strength test value of the SSFRC, and  $f_{cu}$  is the cube compressive strength test value of the SSFRC.

### 3.3. Toughness Evaluation

Figure 7 shows the stress–strain curves of the PC, RC, and SSFRC with different strengths under axial pressure, while Figures 8 and 9 show the variation trends of the tensile and compressive ratios of the SSFRC, respectively. Table 6 shows the tensile compression ratio, folding compression ratio, and toughness index of various concrete types.

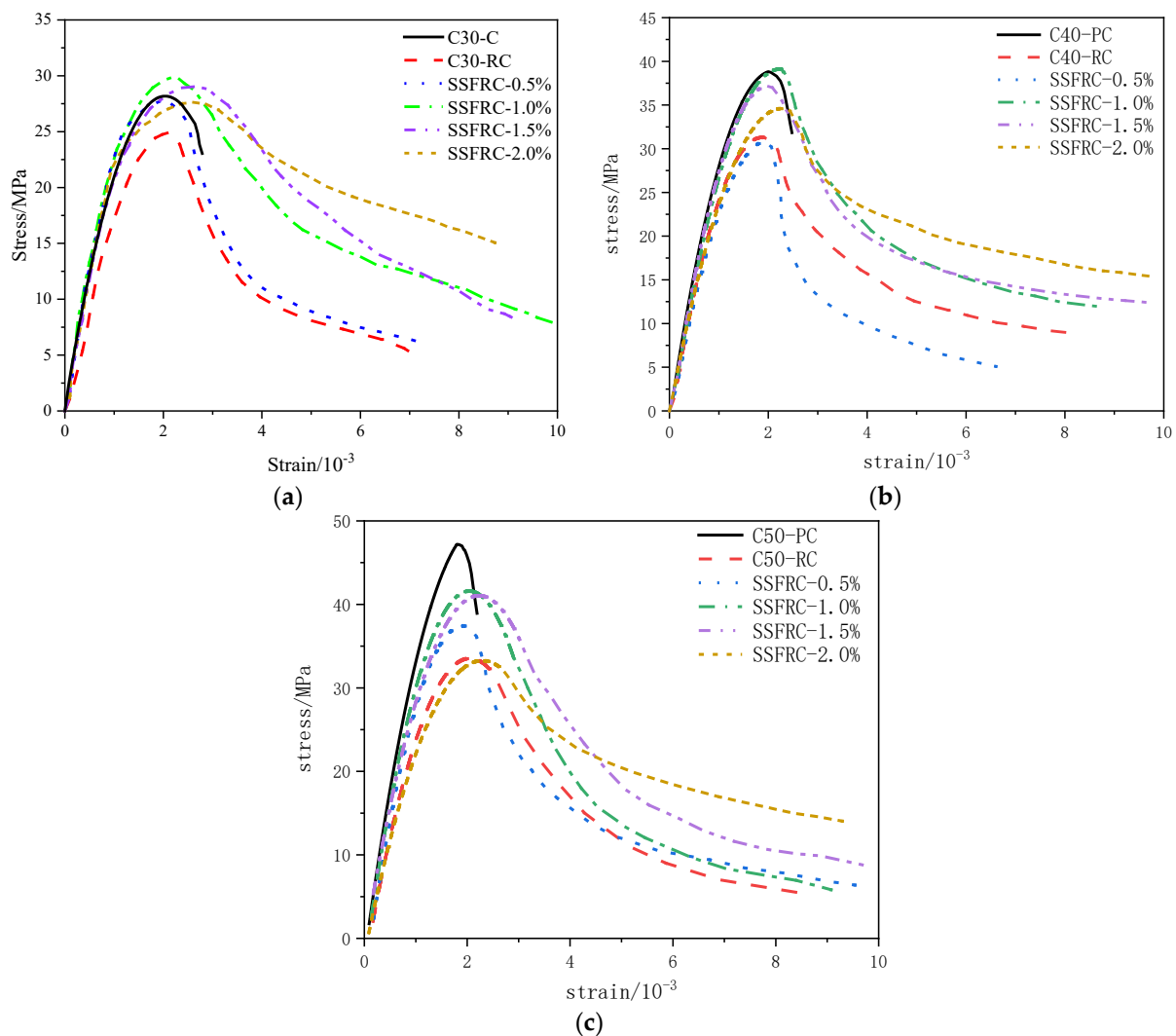


**Figure 7.** Stress–strain curves of different types of concrete: (a) C30; (b) C40; and (c) C50.

As can be seen in Figure 7, the curve was divided into an ascending section (a linear ascending stage before the initial crack point and a nonlinear ascending stage from the initial crack point to the peak stress) and a descending section (a failure stage of the specimen after the peak stress). The full stress–strain curve could be obtained for the RC and SSFRC except for the latter half of the stress–strain curve, which could not be obtained for the PC due to brittle failure. It can be seen from Figure 7a–c that the addition of rubber reduced the peak stress of the PC. This is because rubber reduces the strength of PC, which is the same reason why the compressive strength of the cubes in Section 3.2 decreased.

After adding the RSSF, the peak stress of the specimen first increased and then decreased. This is because after the content of RSSF reaches a certain value, the continuous increase in content will make the RSSF overlap with each other and increase the weak point in the matrix, thus weakening the strengthening effect. The addition of rubber increased

the peak strain of the PC, indicating that rubber can improve the deformation capacity of PC and increase its ductility. After the addition of RSSF, the peak strain of the SSFRC with different matrix strengths increased compared with that of the RC, and the stress–strain area increased with different amplitudes compared with that of the RC. The results show that RSSF has positive effect on RC's crack resistance at different strengths, and the C30 matrix strength was the most significant. With the increase in RSSF content, the decline trend of the post-peak curve was slower than that of the RC, and the compressive toughness of the SSFRC was further improved.

**Table 6.** Tensile compression ratios, folding pressures, and toughness indexes of different types of concrete.

Specimen Number	Tension and Compression Ratio	Flexural Strength and Compressive Strength Ratio	Toughness Index
C30-PC	0.0823	0.13783	-
C30-RC	0.0831	0.13934	1.51
C30-SSFRC-0.5%	0.0926	0.13917	1.48
C30-SSFRC-1.0%	0.0863	0.13521	1.88
C30-SSFRC-1.5%	0.1079	0.16031	1.77
C30-SSFRC-2.0%	0.1058	0.15521	2.05
C40-PC	0.0804	0.12618	-
C40-RC	0.0810	0.12936	1.32
C40-SSFRC-0.5%	0.0927	0.1291	1.75
C40-SSFRC-1.0%	0.0949	0.12758	1.60
C40-SSFRC-1.5%	0.1016	0.14126	1.67
C40-SSFRC-2.0%	0.0997	0.14614	1.97
C50-PC	0.0726	0.11763	-
C50-RC	0.0754	0.12236	1.64
C50-SSFRC-0.5%	0.0824	0.13210	1.72
C50-SSFRC-1.0%	0.0852	0.12419	1.49
C50-SSFRC-1.5%	0.1047	0.14922	1.73
C50-SSFRC-2.0%	0.0967	0.14028	1.98

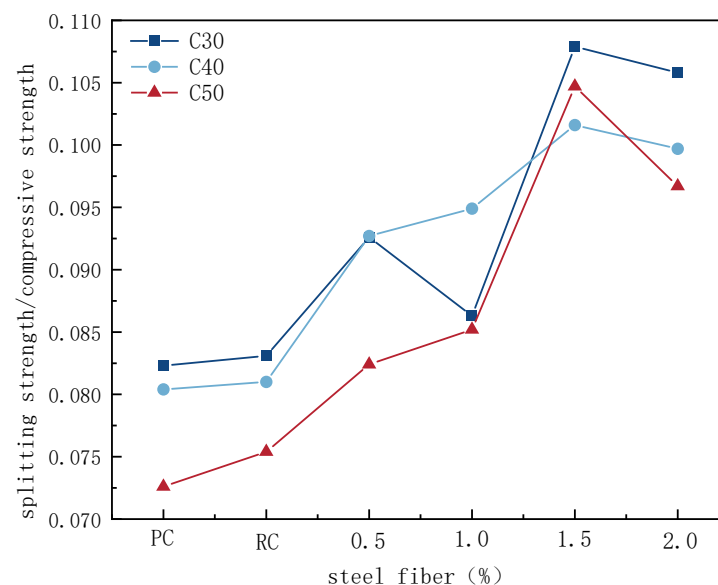


**Figure 8.** Tensile compression ratio curves of different types of concrete.

In Table 5, the compressive strength of the cube is the compressive strength value obtained by testing a cube with a size of  $100 \times 100 \times 100$  mm. This value is mainly used to determine the strength grade of the concrete. The axial compressive strength is the value

obtained by conducting tests on  $100 \times 100 \times 300$  mm test blocks, which is mainly used to determine the design value of the concrete's compressive strength.

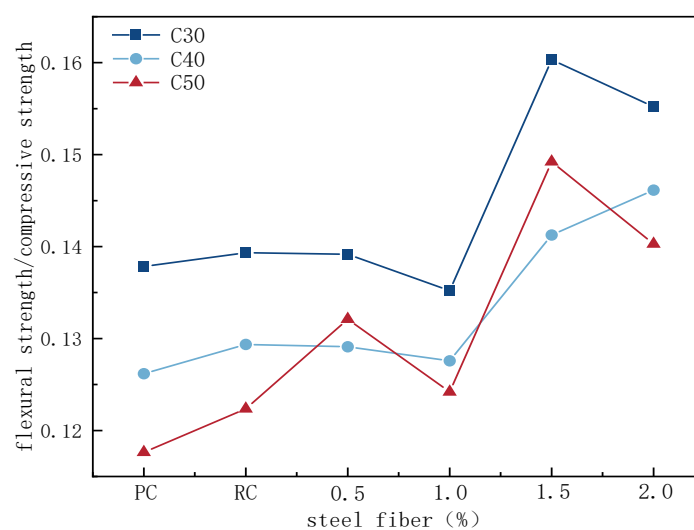


**Figure 9.** Ratio curves of flexural and compressive strengths of different types of concrete.

#### 4. Conclusions

By adding different volumes of RSSF into RC, the mechanical properties and toughness characteristics of RSSF rubber concrete were studied by means of test methods. The main conclusions are as follows:

(1) Rubber particles and different volumes of RSSF will reduce the slump of concrete to a certain extent. The higher the RSSF content, the more the slump decreases. The higher the concrete strength, the lower the slump. But the slump of concrete with a high RSSF content does not decrease continuously.

(2) The addition of rubber particles has similar effects on different mechanical properties of concrete with the same matrix strength. When the matrix strength is different, the mechanical properties of high-strength concrete are affected more. When the RSSF content is 1%, the compressive strength of concrete with different matrix strengths is the best. When the RSSF content is 1.5%, the tensile strength and flexural strength are the best, but the strength improvement effect on high-strength concrete is limited.

(3) Rubber can improve the toughness of PC. The toughness of RC with different matrix strengths is further improved by different dosages of RSSF. When the content of RSSF is 1.5%, the folding ratio and tension ratio of each SSFRC reach the peak value, and the toughness index increases with the increase in the content of RSSF. The synergistic effect of RSSF with rubber particles at a certain amount further increases the toughness of RC. When the content of rubber is 10%, and the content of RSSF is 1.5%, the mechanical properties and compressive toughness of concrete can be improved the most, and the defects of PC brittleness can be effectively improved.

**Author Contributions:** Conceptualization, Q.X.; methodology, M.T.; software, M.P.; validation, H.Z.; formal analysis, J.Y.; investigation, J.Y.; resources, M.T.; data curation, Y.G.; writing—original draft preparation, N.D.; writing—review and editing, J.Y. All authors have read and agreed to the published version of the manuscript.

**Funding:** This research was funded by the National Science and Technology Support Program of China, the National Natural Science Foundation of China, and the State Key Laboratory of Geological Disaster Prevention and Geological Environmental Protection of Chengdu University of Technology under grant numbers 2015BAK09B01, 41877273, and SKLGP2019K019.

**Data Availability Statement:** Data will be made available upon request.

**Acknowledgments:** The authors of the paper would like to thank the editors and reviewers for their guidance and feedback on the paper.

**Conflicts of Interest:** The authors declare that they have no known competing financial interests or personal relationships that could have appeared to influence the work reported in this paper.

## References

1. Straka, P.; Auersvald, M.; Vrtiska, D.; Kittel, H.; Simacek, P.; Vozka, P. Production of transportation fuels via hydrotreating of scrap tires pyrolysis oil. *Chem. Eng. J.* **2023**, *460*, 141764. [[CrossRef](#)]
2. AbdelAleem, B.H.; Ismail, M.K.; Hassan, A.A. The combined effect of crumb rubber and synthetic fibers on impact resistance of self-consolidating concrete. *Constr. Build. Mater.* **2018**, *162*, 816–829. [[CrossRef](#)]
3. Abdelmonem, A.; El-Feky, M.S.; Nasr, E.S.A.; Kohail, M. Performance of high strength concrete containing recycled rubber. *Constr. Build. Mater.* **2019**, *227*, 116660. [[CrossRef](#)]
4. Aly, A.M.; El-Feky, M.S.; Kohail, M.; Nasr, E.S.A. Performance of geopolymer concrete containing recycled rubber. *Constr. Build. Mater.* **2019**, *207*, 136–144. [[CrossRef](#)]
5. Sofi, A. Effect of waste tyre rubber on mechanical and durability properties of concrete—A review. *Ain Shams Eng. J.* **2018**, *9*, 2691–2700. [[CrossRef](#)]
6. Yi, O.; Zhuge, Y.; Ma, X.; Gravina, R.J.; Mills, J.E.; Youssf, O. Push-off and pull-out bond behaviour of crc composite slabs—An experimental investigation. *Eng. Struct.* **2021**, *228*, 111480. [[CrossRef](#)]
7. Siddika, A.; Al Mamun, M.A.; Alyousef, R.; Amran, Y.H.M.; Aslani, F.; Alabduljabbar, H. Properties and utilizations of waste tire rubber in concrete: A review. *Constr. Build. Mater.* **2019**, *224*, 711–731. [[CrossRef](#)]
8. Roychand, R.; Gravina, R.J.; Zhuge, Y.; Ma, X.; Youssf, O.; Mills, J.E. A comprehensive review on the mechanical properties of waste tire rubber concrete. *Constr. Build. Mater.* **2020**, *237*, 117651. [[CrossRef](#)]
9. Richardson, A.; Coventry, K.; Edmondson, V.; Dias, E. Crumb rubber used in concrete to provide freeze–thaw protection (optimal particle size). *J. Clean. Prod.* **2016**, *112*, 599–606. [[CrossRef](#)]
10. Thomas, B.S.; Chandra Gupta, R. Properties of high strength concrete containing scrap tire rubber. *J. Clean. Prod.* **2016**, *113*, 86–92. [[CrossRef](#)]
11. Han, Q.; Yang, G.; Xu, J. Performance of crumb rubber concrete made with high contents of heat pre-treated rubber and magnetized water. *J. Mater. Res. Technol. JMR&T* **2018**, *25*, e2240.
12. Youssf, O.; Swilam, A.; Tahwia, A.M. Application of rubberized cement-based composites in pavements: Suitability and considerations. *Constr. Build. Mater.* **2023**, *23*, 2160–2176.
13. Hassanli, R.; Youssf, O.; Vincent, T.; Mills, J.E.; Manalo, A.; Gravina, R. Experimental Study on Compressive Behavior of FRP-Confined Expansive Rubberized Concrete. *J. Compos. Constr.* **2020**, *24*, 04020034. [[CrossRef](#)]
14. Youssf, O.; Mills, J.E.; Hassanli, R. Assessment of the mechanical performance of crumb rubber concrete. *Constr. Build. Mater.* **2016**, *125*, 175–183. [[CrossRef](#)]
15. Pham, T.M.; Renaud, N.; Pang, V.; Shi, F.; Hao, H.; Chen, W.S. Effect of rubber aggregate size on static and dynamic compressive properties of rubberized concrete. *Struct. Concr.* **2022**, *23*, 2510–2522. [[CrossRef](#)]
16. Abd-Elaal, E.; Araby, S.; Mills, J.E.; Youssf, O.; Roychand, R.; Ma, X.; Zhuge, Y.; Gravina, R.J. Novel approach to improve crumb rubber concrete strength using thermal treatment. *Constr. Build. Mater.* **2019**, *229*, 116901. [[CrossRef](#)]
17. Ismail, M.K.; Hassan, A.A.A. Influence of mixture composition and type of cementitious materials on enhancing the fresh properties and stability of self-consolidating rubberized concrete. *J. Mater. Civ. Eng.* **2016**, *28*, 04015075. [[CrossRef](#)]
18. Ismail, M.K.; Hassan, A.A.A. Use of metakaolin on enhancing the mechanical properties of self-consolidating concrete containing high percentages of crumb rubber. *J. Clean. Prod.* **2016**, *125*, 282–295. [[CrossRef](#)]
19. Abu Bakar, B.H.; Noaman, A.T.; Akil, H.M. Cumulative effect of crumb rubber and steel fiber on the flexural toughness of concrete. *Eng. Technol. Appl. Sci. Res.* **2017**, *7*, 1345–1352. [[CrossRef](#)]
20. Issa, G.A.; Salem, G. Utilization of recycled crumb rubber as fine aggregates in concrete mix design. *Constr. Build. Mater.* **2013**, *42*, 48–52. [[CrossRef](#)]
21. Shahzad, K.; Zhao, Z. Experimental study of NaOH pretreated crumb rubber as substitute of fine aggregate in concrete. *Constr. Build. Mater.* **2022**, *358*, 129448. [[CrossRef](#)]
22. Keshavarz, Z.; Mostofinejad, D. Porcelain and red ceramic wastes used as replacements for coarse aggregate in concrete. *Constr. Build. Mater.* **2019**, *195*, 218–230. [[CrossRef](#)]
23. Ismail, M.K.; Hassan, A.A.A. Impact resistance and mechanical properties of self-consolidating rubberized concrete reinforced with steel fibers. *J. Mater. Civ. Eng.* **2017**, *29*, 04016193. [[CrossRef](#)]
24. Guerra, I.; Vivar, I.; Llamas, B.; Juan, A.; Moran, J. Eco-efficient concretes: The effects of using recycled ceramic material from sanitary installations on the mechanical properties of concrete. *Waste Manag.* **2009**, *29*, 643–646. [[CrossRef](#)] [[PubMed](#)]
25. Gharibi, H.; Mostofinejad, D. Thermal and mechanical properties of concrete containing porcelain ceramic tile waste as fine and coarse aggregates. *Mag. Concr. Res.* **2023**, *75*, 123–134. [[CrossRef](#)]
26. Aggelis, D.G.; Mpalaskas, A.C.; Matikas, T.E. Investigation of different fracture modes in cement-based materials by acoustic emission. *Cem. Concr. Res.* **2013**, *48*, 1–8. [[CrossRef](#)]

27. Xu, J.; Fu, Z.; Han, Q.; Li, H. Fracture monitoring and damage pattern recognition for carbon nanotube-crumb rubber mortar using acoustic emission techniques. *Struct. Control Health Monit.* **2019**, *26*, e2422. [[CrossRef](#)]
28. Han, Q.; Xu, J.; Carpinteri, A.; Lacidogna, G. Localization of acoustic emission sources in structural health monitoring of masonry bridge. *Struct. Control Health Monit.* **2015**, *22*, 314–329. [[CrossRef](#)]
29. Xu, J.; Niu, X.L.; Yao, Z.Y. Mechanical properties and acoustic emission data analyses of crumb rubber concrete under biaxial compression stress states. *Constr. Build. Mater.* **2021**, *298*, 123778. [[CrossRef](#)]
30. Xu, J.; Shu, S.R.; Han, Q.H.; Liu, C. Experimental research on bond behavior of reinforced recycled aggregate concrete based on the acoustic emission technique. *Constr. Build. Mater.* **2018**, *191*, 1230–1241. [[CrossRef](#)]
31. Abouhussien, A.A.; Hassan, A.A.A. Classification of damage in self-consolidating rubberized concrete using acoustic emission intensity analysis. *Ultrasonics* **2020**, *100*, 105999. [[CrossRef](#)] [[PubMed](#)]
32. Ahamad, M.S.S.; Maizul, E.N.M. Digital analysis of geo-referenced concrete scanning electron microscope (SEM) images. *Civ. Environ. Eng. Rep.* **2020**, *30*, 65–79. [[CrossRef](#)]
33. Keshavarz, Z.; Mostofinejad, D. Steel chip and porcelain ceramic wastes used as replacements for coarse aggregates in concrete. *J. Clean. Prod.* **2019**, *230*, 339–351. [[CrossRef](#)]
34. Xu, J.; Niu, X.L.; Ma, Q.; Han, Q.H. Mechanical properties and damage analysis of rubber cement mortar mixed with ceramic waste aggregate based on acoustic emission monitoring technology. *Constr. Build. Mater.* **2021**, *309*, 125084. [[CrossRef](#)]
35. Jimoda, L.A.; Sulaymon, I.D.; Alade, A.O.; Adebayo, G.A. Assessment of environmental impact of open burning of scrap tyres on ambient air quality. *Int. J. Environ. Sci. Technol.* **2018**, *15*, 1323–1330. [[CrossRef](#)]
36. Abd Allah Abd-Elaty, M.; Farouk Ghazy, M.; Hussein Khalifa, O. Mechanical and thermal properties of fibrous rubberized geopolymer mortar. *Constr. Build. Mater.* **2022**, *354*, 129192. [[CrossRef](#)]
37. Wu, Y.F.; Kazmi, S.M.S.; Munir, M.J.; Zhou, Y.; Xing, F. Effect of compression casting method on the compressive strength, elastic modulus and microstructure of rubber concrete. *J. Clean. Prod.* **2020**, *264*, 121746. [[CrossRef](#)]
38. Xie, J.H.; Guo, Y.C.; Liu, L.S.; Xie, Z.H. Compressive and flexural behaviours of a new steel-fibre-reinforced recycled aggregate concrete with crumb rubber. *Constr. Build. Mater.* **2015**, *79*, 263–272. [[CrossRef](#)]
39. Alsaif, A.; Albidah, A.; Abadel, A.; Abbas, H.; Almusallam, T.; Al-Salloum, Y. Behavior of ternary blended cementitious rubberized mixes reinforced with recycled tires steel fibers under different types of impact loads. *Structures* **2022**, *45*, 2292–2305. [[CrossRef](#)]
40. Hilal, N.N. Hardened properties of self-compacting concrete with different crumb rubber size and content. *Int. J. Built Environ. Sustain.* **2017**, *6*, 191–206. [[CrossRef](#)]
41. Stallings, K.A.; Durham, S.A.; Chorzepa, M.G. Effect of cement content and recycled rubber particle size on the performance of rubber-modified concrete. *Int. J. Sustain. Eng.* **2019**, *12*, 189–200. [[CrossRef](#)]
42. Li, Y.; Zhang, S.; Wang, R.; Dang, F. Potential use of waste tire rubber as aggregate in cement concrete—A comprehensive review. *Constr. Build. Mater.* **2019**, *225*, 1183–1201. [[CrossRef](#)]
43. Albidah, A.; Alsaif, A.; Abadel, A.; Abbas, H.; Al-Salloum, Y. Role of recycled vehicle tires quantity and size on the properties of metakaolin-based geopolymer rubberized concrete. *J. Mater. Res. Technol. JMR&T* **2022**, *18*, 2593–2607.
44. Pham, T.M.; Davis, J.; Ha, N.S.; Pournasiri, E.; Shi, F.; Hao, H. Experimental investigation on dynamic properties of ultra-high-performance rubberized concrete (UHPRuC). *Constr. Build. Mater.* **2021**, *307*, 125104. [[CrossRef](#)]
45. Shi, Y.; Long, G.; Ma, C.; Xie, Y.; He, J. Design and preparation of ultra-high performance concrete with low environmental impact. *J. Clean. Prod.* **2019**, *214*, 633–643. [[CrossRef](#)]
46. Tayeh, B.A.; Zeyad, A.M.; Agwa, I.S.; Amin, M. Effect of elevated temperatures on mechanical properties of lightweight geopolymer concrete. *Case Stud. Constr. Mater.* **2021**, *15*, e00673. [[CrossRef](#)]

**Disclaimer/Publisher’s Note:** The statements, opinions and data contained in all publications are solely those of the individual author(s) and contributor(s) and not of MDPI and/or the editor(s). MDPI and/or the editor(s) disclaim responsibility for any injury to people or property resulting from any ideas, methods, instructions or products referred to in the content.